Deep learning models of RNA base-pairing structures make accurate zero-shot predictions of base-base interactions of RNA complexes

Mei Lang[1], Thomas Litfin[2], Ke Chen[1], Jian Zhan[1,3 a], and Yaoqi Zhou[1,2a]

[1]Institute of Systems and Physical Biology, Shenzhen Bay Laboratory, Shenzhen, 518107, China

[2]Institute for Glycomics, Griffith University, Parklands Dr, Southport, QLD 4222, Australia

[3]Ribopeutic Inc, Guangzhou International Bio Island, Guangdong, 510320, China

[a]For correspondence, please email to Dr. Yaoqi Zhou (zhouyq@szbl.ac.cn) or Dr. Jian Zhan (zhanjian@szbl.ac.cn).

ABSTRACT

The intricate network of RNA-RNA interactions, crucial for orchestrating essential cellular processes like transcriptional and translational regulation, has been unveiling through high-throughput techniques and computational predictions. With the emergence of deep learning methodologies, the question arises: how do these cutting-edge techniques for base-pairing prediction compare to traditional free-energy-based approaches, particularly when applied to the challenging domain of interaction prediction via chain concatenation? In this study, we employ base pairs derived from three-dimensional RNA complex structures as the gold standard benchmark to assess the performance of 23 different methods, including recently developed deep learning models. Our results demonstrate that the deep-learning-based methods, SPOT-RNA can be generalized to make accurate zero-shot predictions of RNA-RNA interactions not only between previously unseen RNA structures but also between RNAs without monomeric

structures. The finding underscores the potential of deep learning as a robust tool for advancing our understanding of these complex molecular interactions.

Introduction

Recent advancements in high-throughput techniques have unveiled a complex network of RNA-RNA interactions (RRIs) critical for governing transcriptional and translational processes. These interactions are pivotal in the biogenesis of various RNA molecules, including mRNAs, rRNA, tRNA, microRNAs, and circRNAs[1–3]. Large-scale detection of RRIs has been achieved through innovative approaches that combine cross-linking techniques with high-throughput sequencing. Notably, techniques such as PARIS[4], SPLASH[5], LIGR-seq[6], and COMRADES[7] have employed psoralen or its derivatives, as well as formaldehyde in the case of RIC-Seq[8], for cross-linking. While these methods hold promise, they are not without limitations stemming from probe biases and ligation efficiencies [1–3]. For example, KARR-seq, PARIS, and RIC-seq can only achieve about 55% true positive rate at 20% false positive rate for human 18S rRNA[5]. Furthermore, many of these high-throughput techniques have yet to achieve the single nucleotide resolution.

Attaining the nucleotide-level resolution in RNA structures has historically relied on traditional structure-determination methods such as X-ray crystallography, Nuclear Magnetic Resonance (NMR), and Cryo-electron microscopy. Yet, compared to proteins, determining RNA structures presents formidable challenges due to the unique physiochemical properties of nucleotides and the inherent fragility of RNA structures[9]. This is reflected from the fact that only a meagre 3% of structures in the Protein Data Bank contain RNAs, with even fewer dedicated to RNA-RNA

complexes (681 as of March 16, 2023, before redundancy removal)[10]. This stark contrast becomes even more pronounced when considering the extensive collection of more than 31 million noncoding RNA sequences catalogued in the RNAcentral database [11]. Given the cost and challenges associated with experimental approaches, there is an imperative need for development of complementary computational prediction techniques.

The existing methods for predicting RNA-RNA interactions (RRIs) can be broadly classified into alignment-based, free-energy-based, and homology modeling approaches[12,13]. Alignment-based techniques, such as GUUGle[14] and RIsearch[15], focus on inter-RNA base pairs while overlooking potential intra-RNA interactions. Free-energy-based methods can be categorized into those considering only intermolecular interactions for expediency (such as RNAhybrid[16], RNAduplex[17], RNAplex-c[18], and DuplexFold[19]), those factoring in intramolecular interactions based on solvent accessibility (such as RNAup[20], IntaRNA[21], RNAplex-a[22], and AccessFold[23]), and those accommodating both intra- and inter-molecular base pairs through sequence concatenation (such as PAIRFOLD[24], RNAcofold[25] and biFold[19]) or without restrictions (such as RactIP[26]). Homology-based techniques, exemplified by TargetRNA2[27], CopraRNA[28], RNAaliduplex[17] and PETcofold[29], utilize evolutionary information to infer binding.

Presently, 'de novo' RRI prediction methods predominantly rely on free-energy-based approaches, limited by their approximate energy or scoring functions, akin to the challenges faced in RNA secondary structure prediction[30]. Recent advancements have seen the emergence of deep learning-based methods, starting with SPOT-RNA[31], which achieved the first end-to-end

prediction of intra-RNA base pairs. Subsequent developments include mxfold2[32], UFold[33], and 2dRNA[34]. To further enhance prediction accuracy, SPOT-RNA2[35] was developed to integrate evolutionary profiles and mutational coupling data generated by RNAcmap[36] .

In this study, we conducted a comprehensive benchmark of various methods for predicting inter-RNA interactions. Our evaluation encompassed traditional energy-based techniques and newly developed deep learning models based on simple sequence concatenation. To ensure a rigorous assessment, we employed base pairs derived from experimentally-determined RNA-RNA complex structures and eliminated monomer structures employed for training of SPOT-RNA and SPOT-RNA2 through a strict structural similarity cutoff (TM-score[37] <0.3), in addition to sequence similarity cut off by CD-HIT. This challenging set of the complex of unseen structures revealed significant improvements of SPOT-RNA's performance over the other 22 methods evaluated, underscoring the transferability of deep learning from intra-RNA to inter-RNA interaction prediction. The performance by SPOT-RNA is robust against different types of RNA complexes. Further tests on training-family-excluded test sets confirm the robustness of SPOT-RNA in heterodimeric complexes of RNAs, in particular.

Results

Method Comparison on Inter-RNA Base Pair Prediction

In this study, we compared 23 different RRI predictors on a benchmark set of 64 RNA-RNA pairs after excluding all monomer structures remotely similar to the RNA structures employed in the training and validation sets for SPOT-RNA and SPOT-RNA2. We evaluated their performance in

86 untrained inter-RNA base pair prediction through precision/recall curves and F1 score
87 distributions, as shown in Figure 1. The performance metrics, including overall F1-score,
88 Mathews' correlation coefficient (MCC) values, and the median F1-score and standard deviation
89 of individual RNA pairs, are also summarized in Table 1. Predictors with probabilistic outputs are
90 represented by precision-recall (PR) curves, while others are represented as single points. For all
91 methods with chain concatenation for predicting RNA-RNA interactions, a low case "c" is
92 appended to the method name. They are RNAfoldc, UFoldc, MXfold2c, EternaFoldc, SPOT-RNAc,
93 and SPOT-RNA2c. No linker was employed because adding a 3-nucleotide link did not lead to
94 performance improvement (See Methods).
95
96 As shown in Figure 1A, SPOT-RNA2c is the most accurate predictor at low sensitivity (<0.2).
97 However, the overall PR curve given by SPOT-RNAc has the best performance. We can also
98 measure the performance by the overall F1-Score for all RNA pairs and the median F1-Score for
99 individual RNA pairs. The thresholds for determining F1-scores of SPOT-RNAc and SPOT-RNA2c in
100 the test set were set according to the thresholds for producing the highest F1-scores in the
101 validation dataset for SPOT-RNAc and SPOT-RNA2c, respectively. Table 1 confirmed the result
102 from the PR curve that SPOT-RNAc achieved the best overall performance with an overall F1-
103 Score of 0.583, outperforming SPOT-RNA2c (the overall F1-Score of 0.561) and EternaFold (F1-
104 Score of 0.512). SPOT-RNAc improves over SPOT-RNA2c by more than 4% and outperforms other
105 methods by over 14%, a pattern similarly observed in MCC values (Table 1).
106

107 Figure 1B presents the distribution of F1 scores for individual RNA pairs, including median, 25th,

108 and 75th percentiles. SPOT-RNAc continues to achieve the best performance with the highest

109 median F1 score of 0.582, outperforming the next best SPOT-RNA2c (median F1-score of 0.533)

110 with a 10% improvement. The improvement of SPOT-RNAc over all methods are statistically

111 significant except EternaFold (Table 1).

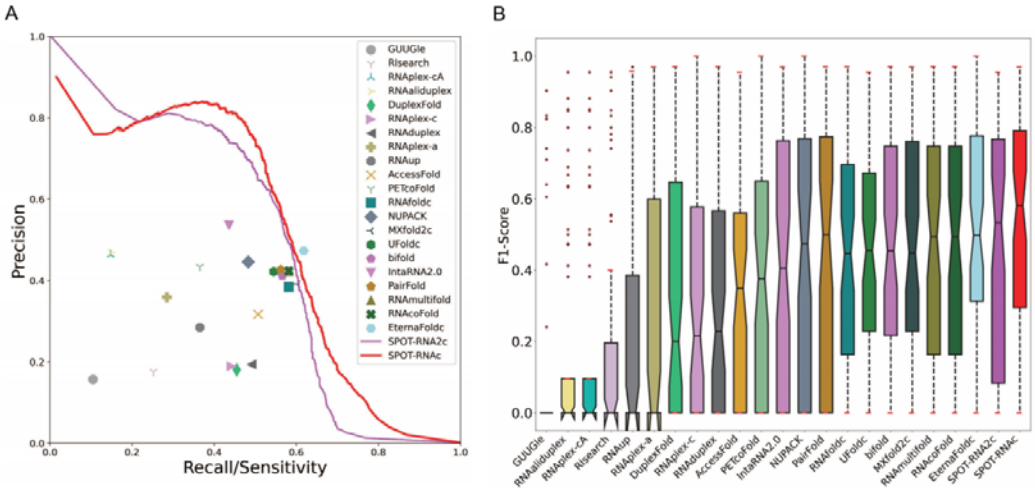

112

113 Figure 1: Performance comparison of 23 methods for inter-RNA base-pair prediction on the 64

114 complexes of RNA structures unseen by SPOT-RNA and SPOT-RNA2. All structures in the test set

115 have the structural similarity score TM-Score<0.3 compared to the monomeric structures used in

116 training and validating SPOT-RNA and SPOT-RNA2 methods. (A) Precision-recall curves (for those

117 methods with probabilistic outputs) or points given by 23 methods (B) Distribution of F1 scores

118 for inter-RNA base pair prediction for individual RNA pairs by the same 23 methods. Each boxplot

119 shows the median, 25th, and 75th percentiles, with outliers represented by "•". SPOT-RNAc

120 exhibits the best performance for both overall and individual measures of F1-scores.

121

122 Table 1: Performance Comparison of 23 Predictors of Inter-RNA Base Pairs on 64 Complexes of

123 RNA Structures Unseen by SPOT-RNA and SPOT-RNA2. All single-chain structures in the test set

have the structural similarity score TM-Score<0.3 compared to the monomeric structures used in training and validating SPOT-RNA and SPOT-RNA2 methods.

Methods	PPV/ Precision	Sensitivity/Recall	Overall F1-Score	MCC	Individual F1-Score Median ± Std	P-value
GUUGle	0.157	0.105	0.126	0.124	0.000 ± 0.241	$7.90e^{-15}$
RIsearch	0.176	0.252	0.207	0.205	0.000 ± 0.319	$2.03e^{-12}$
RNAplex-cA*	0.463	0.148	0.224	0.259	0.000 ± 0.296	$1.56e^{-11}$
RNAaliduplex*	0.469	0.148	0.225	0.261	0.000 ± 0.296	$1.56e^{-11}$
DuplexFold	0.181	0.455	0.259	0.281	0.200 ± 0.344	$6.12e^{-08}$
RNAplex-c	0.189	0.442	0.265	0.283	0.216 ± 0.343	$1.10e^{-08}$
RNAduplex	0.194	0.491	0.278	0.303	0.229 ± 0.329	$8.49e^{-09}$
RNAplex-a	0.359	0.285	0.318	0.316	0.000 ± 0.331	$1.43e^{-09}$
RNAup	0.285	0.365	0.320	0.318	0.000 ± 0.342	$4.13e^{-12}$
AccessFold	0.317	0.507	0.390	0.397	0.349 ± 0.315	$6.05e^{-06}$
PETcoFold*	0.434	0.365	0.397	0.395	0.376 ± 0.352	$9.24e^{-05}$
RNAfoldc	0.384	0.582	0.463	0.469	0.446 ± 0.318	0.007
NUPACK	0.446	0.483	0.464	0.461	0.474 ± 0.355	0.001
MXfold2c	0.391	0.603	0.474	0.482	0.448 ± 0.320	0.004
UFoldc	0.422	0.545	0.476	0.476	0.455 ± 0.302	0.002
bifold	0.412	0.566	0.477	0.480	0.454 ± 0.325	0.014
IntaRNA2.0	0.536	0.436	0.481	0.481	0.405 ± 0.377	$9.75e^{-05}$
PairFold	0.427	0.562	0.485	0.486	0.500 ± 0.339	0.007
RNAmultifold	0.423	0.582	0.490	0.493	0.494 ± 0.325	0.015
RNAcoFold	0.424	0.582	0.491	0.494	0.494 ± 0.325	0.015
EternaFoldc	0.473	**0.618**	0.512	0.519	0.498 ± 0.314	0.088
SPOT-RNA2c*	0.583	0.540	0.561	0.559	0.533 ± 0.331	0.012
SPOT-RNAc	**0.620**	0.551	**0.583**	**0.583**	**0.582** ± 0.326	

126 Note: The overall F1-score is harmonic mean of precision and recall for all RNA pairs. PPV denotes

127 positive predictive value. MCC denotes Matthews' correlation coefficient. The star * denotes the

128 use of evolution information. Methods with an ending of "c" indicate the use of chain

129 concatenation for RNA-RNA interaction prediction. Median F1 means the median F1 value of

130 single RNA. The P-value of a given method was computed by against the result from SPOT-RNAc.

131 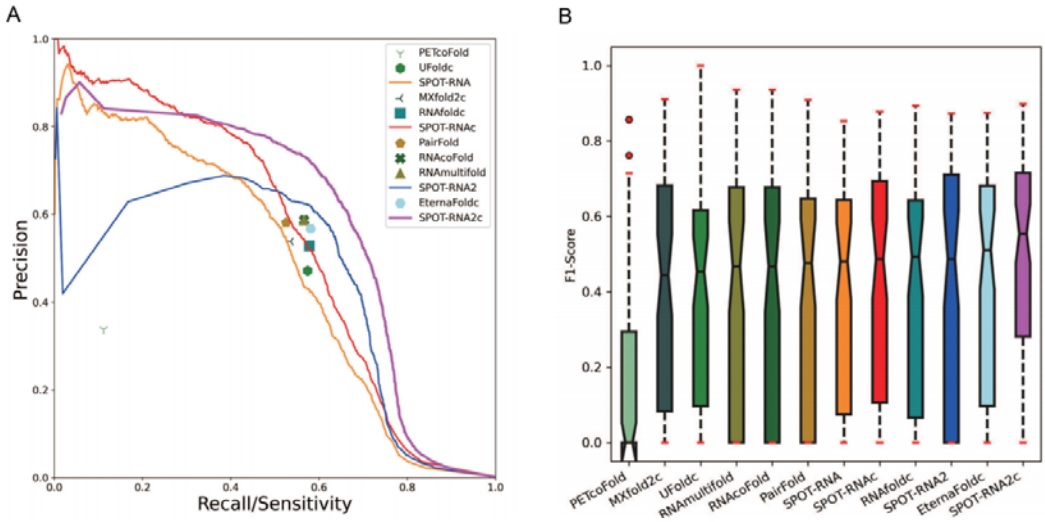

132 Figure 2: Performance Comparison of Intra-RNA Base Pair Prediction by 12 methods (A) Precision-

133 recall curves and points illustrate the performance rankings. (B) A distribution of F1-scores for

134 intra-RNA base pair prediction. SPOT-RNA and SPOT-RNAc represent intramolecular base pair

135 prediction as single and concatenated chains, respectively. Evolution-based SPOT-RNA2c (or

136 SPOT-RNA2) outperforms SPOT-RNAc (or SPOT-RNA) for intra-RNA base pairs.

137

138 It's important to assess how these methods perform on intra-molecular interactions, although

139 not all RRI methods offer predictions for such interactions. We remove these RNAs without intra-

140 base-pairing structures. This leads to 77 RNA chains. Figure 2A compares the PR curves or PR

141 points given by 12 methods. Interestingly, PR curves indicate that SPOT-RNA2c now has the best

142 performance. The overall performance according to overall F1-scores given by SPOT-RNA2c (Table

143 2) is the highest, surpassing the next best methods (SPOT-RNA2 without chain concatenation) by

144 a 6% improvement in F1-score, and the third best (RNAmultifold or RNAcoFold) by 12%, with

145 SPOT-RNAc ranking as the fifth best. This trend is consistent with MCC values.

146

147 Table 2: Performance Comparison of 12 Predictors for Predicting Intra-RNA Base Pairs on 77

148 unseen RNA structures that have intra secondary structure in 64 RNA-RNA Complex Structures.

Methods	PPV/ Precision	Sensitivity /Recall	Overall F1-Score	MCC	Individual F1-Score Median ± Std	P-value
PETcoFold*	0.338	0.112	0.168	0.194	0.000 ± 0.217	$1.62e^{-15}$
UFoldc	0.471	0.574	0.517	0.519	0.452 ± 0.278	$5.33e^{-07}$
SPOT-RNA	0.584	0.486	0.531	0.531	0.476 ± 0.271	$1.51e^{-06}$
MXfold2c	0.538	0.536	0.537	0.536	0.444 ± 0.291	0.0001
RNAfoldc	0.528	0.578	0.552	0.551	0.494 ± 0.287	$1.06e^{-05}$
PairFold	0.581	0.525	0.552	0.551	0.483 ± 0.308	$8.15e^{-05}$
SPOT-RNAc	0.653	0.493	0.562	0.567	0.481 ± 0.291	0.0005
EternaFoldc	0.567	0.581	0.574	0.573	0.511 ± 0.294	0.001
RNAcoFold	0.587	0.566	0.576	0.576	0.467 ± 0.305	0.001
RNAmultifold	0.587	0.566	0.576	0.576	0.467 ± 0.305	0.001
SPOT-RNA2*	0.589	0.629	0.608	0.607	0.489 ± 0.310	0.007
SPOT-RNA2c*	**0.626**	**0.665**	**0.645**	**0.644**	**0.560 ± 0.294**	-

149 Note: The overall F1-score is harmonic mean of precision and recall for all RNA pairs. PPV denotes

150 positive predictive value. MCC denotes Matthew's correlation coefficient. The star * indicates the

151 use of evolution information. Std means standard deviation. Median F1 means the median F1

152 value of individual RNA chains. The P-value of a given method is calculated by against the result

153 of SPOT-RNA2c.

154

155 Figure 2B further examines the distribution of F1-scores for individual RNAs. SPOT-RNA2c

156 continues to lead with the highest median F1-score at 0.560, while EternaFold follows closely

157 with the second-best median F1-score of 0.511. The differences in F1-score distributions between

158 SPOT-RNA2c and other methods are all statistically significant, with a p-value of 0.001 when

159 comparing SPOT-RNA2c to the second best EternaFold (Table 2).

160

161 Intuitively, a better intra-RNA base-pairing prediction should lead to a better inter-RNA base-

162 pairing prediction. However, although SPOT-RNA2c has the best performance for intra-RNA

163 interaction prediction, it is SPOT-RNAc with the best performance for inter-RNA interaction

164 prediction. If we remove these RNA RRI pairs of which both chains do not have intra-base-pairing

165 structures, this leads to 53 RRI pairs. Figure 3A compares intermolecular F1-scores for individual

166 RNA pairs from SPOT-RNAc with the average intramolecular F1-scores. No correlation was found.

167 Similar uncorrelated intra- and inter-RNA F1-scores are observed for SPOT-RNA2c (Figure 3B).

168 This suggests that the evolution information contained in SPOT-RNA2c did contain the co-

169 evolution information for predicting intra-RNA, but not inter-RNA interactions.

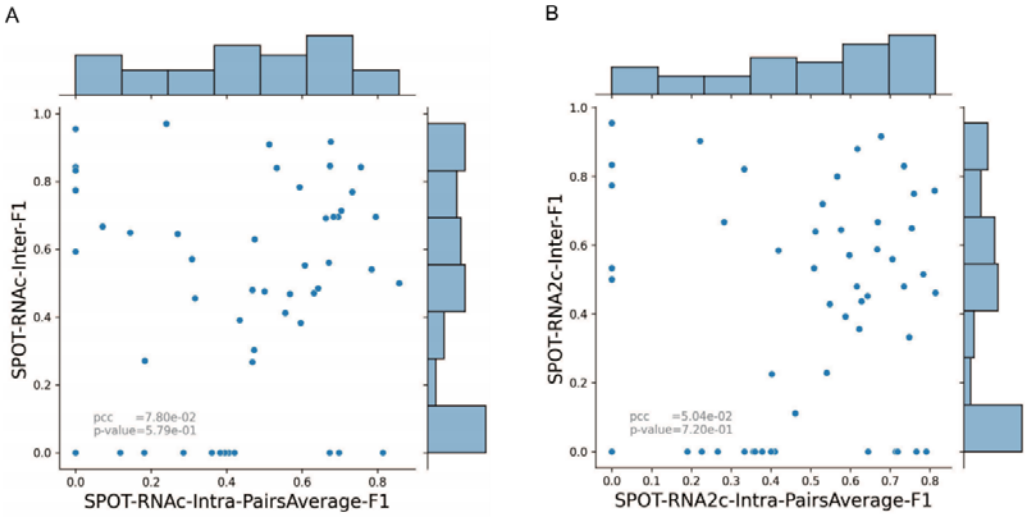

Figure 3 No Correlation between Inter-RNA F1-scores and Intra-RNA F1-scores. (A) Inter-RNA F1-scores versus the average Intra-RNA F1-scores of SPOT-RNAc for 53 RNA complex structures with intra-RNA base pairs for both chains. (B) Inter-RNA F1-scores versus Intra-RNA F1-scores of SPOT-RNA2c for 53 RNA complex structures.

We also assessed the impact of sequence concatenation on the intra-RNA base-pair prediction (i.e., SPOT-RNA versus SPOT-RNAc, SPOT-RNA2 versus SPOT-RNA2c). Table 2 shows that SPOT-RNAc/SPOT-RNA2c are better than SPOT-RNA/SPOT-RNA2 based on either overall F1-score or the median of individual F1-scores. In both cases, the difference is statistically significant with a p-value of 0.0007 between SPOT-RNA and SPOT-RNAc and a p-value of 0.007 between SPOT-RNA2 and SPOT-RNA2c. This indicates that knowing the binding partner improves the intra-RNA base pair prediction.

We observed that some inter-RNA (and intra-RNA) interactions were predicted with F1 score of 0 as shown in Figures 3A and 3B. To understand the reason behind these poor predictions, we

186 examined F1-scores given by SPOT-RNAc as a function of sequence length (L1+L2) in Figure 4A.

187 No obvious correlation was found. However, when we plotted F1-scores against the number of

188 true inter-RNA base pairs divided by the square root of (L1*L2), a clear and strong correlation

189 emerged with a Pearson's correlation coefficient (PCC) of 0.464 (Figure 4B). Thus, poor

190 predictions, including those with F1-scores of 0, can be attributed to the scarcity of inter-RNA

191 contacts relative to the sequence lengths. This observation holds true for intra-RNA base pair

192 prediction as well: intra-RNA interactions with F1-scores of 0 also involve very few intra-RNA base

193 pairs (<5).

194 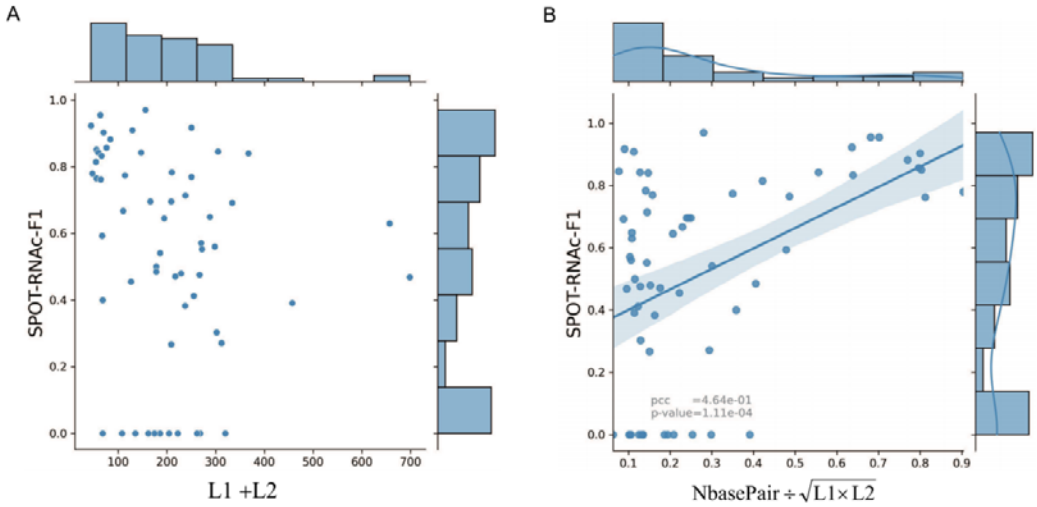

195 Figure 4: Relationship Between Inter-RNA Base Pairing Prediction and Sequence/Interaction

196 Characteristics. (A) The inter-RNA F1 scores for individual RNA-RNA complexes from SPOT-RNAc

197 plotted against the sum of sequence lengths (L1+L2). (B) The inter-RNA F1 scores for individual

198 RNA-RNA complexes from SPOT-RNAc plotted against the normalized number of inter-RNA base

199 pairs (the number of true inter-RNA base pairs divided by the $\sqrt{L1 \times L2}$). The performance does

200 not correlate with sequence length but is related to the normalized number of inter-RNA base

201 pairs.

202

203 One question is whether the method performance depends on RNA types. We classified 64
204 complexes into rRNA-containing complexes (only 8), snRNA/snoRNA/mRNA-containing complexes
205 (40), and RNA complexes lacking intra-RNA interactions (16). SPOT-RNAc is consistently the best
206 in each category as shown Supplementary Table S2 for the overall F1-score and MCC values. It is
207 of note that even for RNA complexes lacking intra-RNA interactions (i.e. these extreme cases of
208 unstructured RNAs are not employed for training in neither SPOT-RNA, nor SPOT-RNA2), SPOT-
209 RNAc continues to provide the best overall F1-score and MCC values, although its performance
210 for averaging over individual complexes is statistically similar to the those of some energy-based
211 techniques. The consistency of SPOT-RNAc performance among different RNA types
212 demonstrates that deep learning, even with a limited number of 3D structures for training, can
213 yield generalizable models for inter-RNA base pair prediction.
214
215 Despite the attempt to remove structural homologs from training by structural alignment, some
216 RNA families in training sets (rRNA and spliceosome complexes) were still included in the above
217 64-complex test sets because RNAs in the same family do not necessarily have an identical
218 structure. We further examined the effect of excluding-training families in intra-base pair
219 prediction by establishing new datasets. They were obtained by removing training/validation
220 families from 64 test complexes and locating additional new RNA complexes (up to 2024/02/28)
221 (See methods). These two datasets are mixed and separated into 15 hetero dimeric complexes
222 and 13 homo-dimeric complexes. For 15 hetero-dimer complexes, although the difference
223 between SPOT-RNAc and some methods are statistically insignificant, SPOT-RNAc remains the
224 best performance among all the methods compared for the overall performance (Table 3),

225 whereas SPOT-RNA2 remains the best for intra-RNA base-pair prediction (Supplementary Table
226 S3) with an overall F1-score of 0.589, followed by RNAmultifold (0.586) and RNAcoFold (0.586). If
227 ranked by median F1-score, SPOT-RNA2c remains the best for intra-RNA interaction predition.
228 Most did poorly with a median F1-score of 0 except SPOT-RNA2c, due to low number of intra-
229 RNA contacts for this set of the data. All also did very poorly with median F1-score of 0 for inter-
230 RNA base-pair prediction in the 13-homodimer set (Supplementary Table S4), whereas SPOT-
231 RNA2 is the best performance with an overall F1-score of 0.750, followed by SPOT-RNA (0.587)
232 and RNA-RNA2c (0.529) for intra-RNA base-pair prediction (Supplementary Table S5).
233
234 Table 3 Performance comparison of all predictors on 15 hetero-dimer complexes of inter-RNA
235 base pairs that are not in RNA families containing in TR0/VL0 (bpRNA) and TR1/VL1 for training
236 SPOT-RNA and SPOT-RNA2.

Methods	PPV/ Precision	Sensitivity/Recall	Overall F1-Score	MCC	Individual F1-Score Median ± Std	P-value
GUUGle	0.433	0.318	0.367	0.367	0.000 ± 0.355	$9.06e^{-05}$
RNAaliduplex*	0.647	0.331	0.438	0.460	0.381 ± 0.359	0.0005
RNAplex-cA*	0.647	0.331	0.438	0.460	0.381 ± 0.359	0.0005
RNAup	0.464	0.764	0.577	0.592	0.615 ± 0.227	$3.35e^{-06}$
RIsearch	0.472	0.744	0.578	0.589	0.781 ± 0.347	0.0399
RNAduplex	0.469	0.807	0.593	0.611	0.846 ± 0.301	0.1529
RNAplex-a	0.676	0.561	0.613	0.613	0.652 ± 0.271	0.0014
PETcoFold*	0.684	0.561	0.616	0.617	0.638 ± 0.306	0.0092
DuplexFold	0.559	0.780	0.651	0.657	0.846 ± 0.313	0.1867
RNAplex-c	0.572	0.780	0.660	0.665	0.846 ± 0.313	0.1867

PairFold	0.634	0.807	0.710	0.713	0.846 ± 0.283	0.2091
UFold	0.659	0.793	0.720	0.721	0.833 ± 0.274	0.1352
bifold	0.684	0.793	0.734	0.734	0.846 ± 0.278	0.2157
RNAfoldc	0.672	0.820	0.739	0.740	0.833 ± 0.273	0.1101
NUPACK	0.698	0.797	0.744	0.744	0.846 ± 0.271	0.3273
EternaFoldc	0.684	0.816	0.744	0.745	0.833 ± 0.269	0.0099
RNAmultifold	0.702	0.797	0.746	0.746	0.846 ± 0.276	0.1303
RNAcoFold	0.702	0.797	0.746	0.746	0.846 ± 0.276	0.1303
SPOT-RNA2c*	0.721	0.787	0.753	0.751	0.821 ± 0.269	0.0713
IntaRNA2.0	0.713	0.800	0.754	0.753	**0.846** ± 0.272	0.3950
MXfold2	0.684	**0.839**	0.754	0.756	0.833 ± 0.210	0.5833
AccessFold	0.696	0.826	0.755	0.756	0.833 ± 0.221	0.4844
SPOT-RNAc	**0.745**	0.823	**0.782**	**0.781**	0.833 ± 0.247	-

Note: The overall F1-score is harmonic mean of precision and recall for all RNA pairs. PPV denotes positive predictive value. MCC denotes Matthews' correlation coefficient. The star * denotes the use of evolution information. Methods with an ending of "c" indicate the use of chain concatenation for RNA-RNA interaction prediction. Median F1 means the median F1 value of F1 values for single RNAs. The P-value of a given method was calculated by against the result from SPOT-RNAc

We selected one example to illustrate SPOT-RNA's performance in RRI prediction. Figure 4A displays predicted and actual base-pairing maps for the subunits L2a rRNA complexed with L3b rRNA from Chlamydomonas reinhardtii mitoribosome (PDB ID 7PKT, chain ID 2 and chain ID 3). Figure 5A displays the intra- and inter-base-pairing maps of these two RNAs with Figure 5B for

inter-base-pairing maps only. The F1 scores for intra-RNA base pairs are 0.32 for L2a rRNA and 0.30 for L3b rRNA, while the F1-score for inter-RNA base pairs is 0.571. Correctly predicted base pairs are highlighted with red dots in Figures 5B and 5C, and their 3D locations were shown as red-colored bases in Figure 5C. For this complex structure, precision for inter-RNA base pairs is 0.435, and sensitivity is relatively high (0.769).

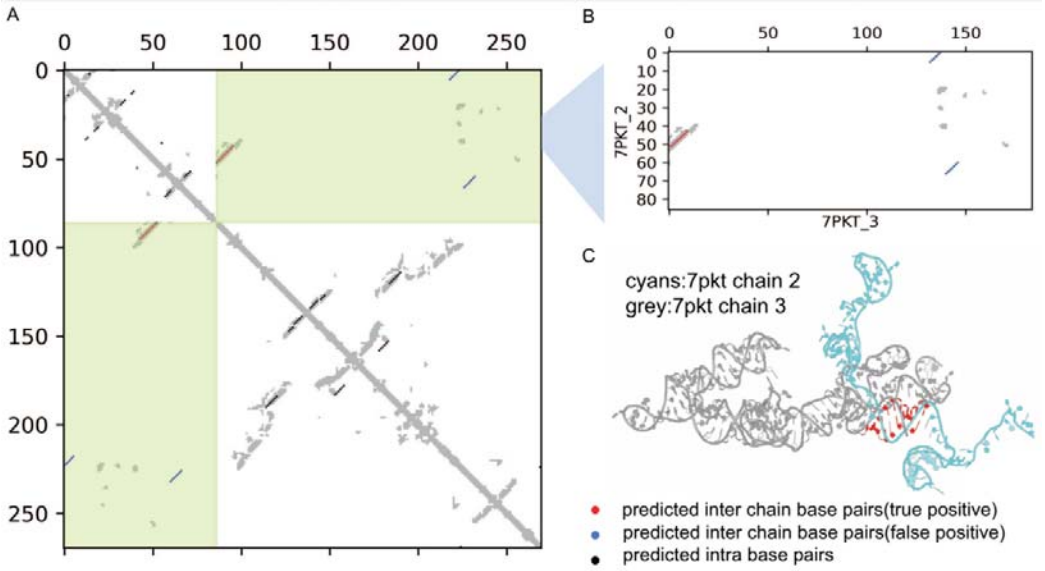

Figure 5: Accurate Prediction of Key Inter-RNA Base-pairing Contacts in RNA Complexes by SPOT-RNAc. Complex structure of large subunits of the Chlamydomonas reinhardtii mitoribosome (L2aRNA and L3bRNA in PDB ID 7PKT) with true distance-contact map and predicted intra and inter-RNA base pairs (A), inter-RNA base pairs only (B), and 3-D structure (C). Predicted intra-base pairs and inter-base pairs are denoted by black and red dots, respectively, in the base-pairing maps. In the 3-D structure (C), correctly predicted inter-RNA base pairs are highlighted in red.

Discussion

This study represents a comprehensive benchmark for assessing more than 20 methods in predicting RNA-RNA interactions. Previous benchmarks were constrained to interactions involving

263 small RNAs without intra-RNA base pairs. For instance, Lai and Meyer [13] compared 14 RRI
264 methods based on experimentally confirmed interactions in fungal snoRNA-rRNA and bacterial
265 sRNA-mRNA pairs. Umu and Gardner[12] examined 15 RRI methods using a dataset focused on
266 short linear base-pair matching. Antonov et al.[38] compared 13 RRI methods on mammalian
267 lncRNAs with experimentally proven hybridizations. In contrast, our study presents the first
268 comprehensive benchmark of 23 RRI prediction methods using known RRI interactions derived
269 from 3D structures at the base pair level. Notably, most of these complexes (53/64) include RNAs
270 with 3D structures and intra-RNA base pairs. Additionally, this study marks the first inclusion of
271 deep-learning based methods for comparisons, utilizing chain concatenation.
272
273 In contrast to proteins, the available non-redundant data for RNA structures is limited. This raises
274 concerns about the generalizability of deep learning models trained on such limited data.
275 Previous studies by Szikszai et al [39] and Qiu [40] highlighted the challenges of deep-learning models
276 when applied to unseen families not present in the training and validation sets. SPOT-RNA and
277 SPOT-RNA2 were initially trained with a set of bpRNA dataset after removing all sequences in
278 bpRNA with known 3D structures by CD-HIT (80% sequence identity cut-off), followed by transfer
279 learning with 3D-structure-derived base pairs. To evaluate the adaptability of SPOT-RNA and
280 SPOT-RNA2 beyond their training and validation data, we placed them to the test of untrained
281 inter-RNA interactions. To avoid possible “over-trained” intra-RNA interactions affecting
282 prediction of inter-RNA interactions, we excluded all single-chain structures in the complex test
283 set with the structural similarity score (TM-score)≥0.3, compared to those in the training and
284 validation sets of SPOT-RNA. Interestingly, the performance of intra-RNA base-pair prediction

285 does not correlate with the performance of inter-RNA base-pair prediction (Figure 3A). Lacking
286 correlation suggests that the performance for predicting inter-RNA interactions is independent of
287 the performance for predicting intra-RNA interactions and the dataset for inter-RNA interactions
288 can be employed as an independent test set for the methods trained for predicting intra-RNA
289 interactions. Despite the above precaution, training/validation families were not entirely
290 excluded because RNAs in the same family may not have an identical structure. Thus, we further
291 established two family-excluded test sets (15 hetero-dimeric RNAs and 13 homo-dimeric RNAs).
292 SPOT-RNA and SPOT-RNA2 remain best performance for inter and intra-RNA base-pair prediction,
293 respectively, except for inter-base-pair prediction for homodimeric RNAs, for which no methods
294 did well. The generalization capability of SPOT-RNA is further illustrated with its robust
295 performance across different RNA types, even for RNAs with few intra-RNA structures
296 (Supplementary Table S2).
297
298 SPOT-RNA2, which incorporates evolution and co-evolution information, outperforms SPOT-RNA
299 for intra-RNA base pairs, aligning with previous findings (Table 2) [35]. However, SPOT-RNA2c
300 underperforms SPOT-RNAc for inter-RNA base pairs. Notably, SPOT-RNA2 exhibits a positive
301 correlation with the number of effective homologous sequences for intra-RNA base-pair
302 prediction (PCC=0.5, p-value=2×10^{-6}, Supplementary Figure 1C), but this correlation nearly
303 diminishes for SPOT-RNA2c for intra-RNA base pairs (PCC=0.27, p-value=0.05) and turned
304 negative for inter-RNA base pair prediction (PCC=-0.3, p-value=0.02). This suggests that using
305 linked sequences in SPOT-RNA2c for homology search may have provided harmful information
306 for inferring inter-RNA interactions. In the future, it may be necessary to utilize sequences from

307 the same species for homology searches, as co-evolution information can only be detected
308 through inter-species comparisons via Multiple Sequence Alignment (MSA) pairing as has been
309 done for proteins[41]. However, the failure of SPOT-RNA2 in predicting inter-RNA interactions
310 between homodimers indicates that the coevolution signals between RNAs may be too weak to
311 capture.
312
313 For predicting RNA-RNA interactions, we concatenated two chains (A and B) as a single chain. To
314 eliminate artificial sequence-order dependence, we predicted results for both AB and BA chains
315 and then calculated the average. Interestingly, we found that in some cases, one sequence order
316 (e.g., BA) outperformed the other (i.e., AB). Upon closer examination, we discovered for some
317 RNA pairs that the order with a shorter separation in sequence positions for contacting base pairs
318 tended to perform better. This observation is intuitive, as longer-range interactions are inherently
319 more challenging to predict. However, there were some outliers deserving further studies.

320 Methods

321 **Benchmark datasets**

322 We retrieved all RNA structures from the Protein Data Bank (PDB) in March 2023[10] and
323 specifically selected structures featuring two RNA chains with a minimum of 5 inter-RNA base
324 pairs. The identification of base pairs was carried out using DSSR[42]. For the base-pair prediction in
325 complex structures, interacting base pairs inside the complex are positive samples, and unpaired
326 bases between them are naturally classified as negative samples. To eliminate redundancy, we

327 applied CD-HIT-EST[43], removing binding pairs with over 80% sequence identity between either

328 chain. This initial step resulted in 155 unique RNA-RNA interaction (RRI) pairs.

329

330 To ensure stringency, we further filtered out RRI pairs that exhibited single-chain structural

331 similarities with any RNAs in the SPOT-RNA training set, defined by TM-score ≥0.3 using RNA-

332 align[44] with the length of the query sequence for normalization. This rigorous process yielded a

333 final benchmark set comprising 64 unique RRI pairs. The PDB IDs of the benchmark set can be

334 found in Supplementary Table S6. To further build a dataset excluding RNA families employed in

335 training/validating SPOT-RNA, we identified 14 complexes out of 64 test complexes whose RNAs

336 do not belong to any RFAM families with RNAs contained in training/validation TR0/VL0 (bpRNA)

337 and TR1/VL1 (RNAs with 3D structures) sets of SPOT-RNA.

338

339 To expand this dataset, we re-downloaded all RNA complexes on 2024/02/28 from the protein

340 data bank and processed by DSSR. Potential complexes were extracted from asymmetric units

341 and biological assemblies and then filtered such that only structures with 6 or more

342 intermolecular and 3 or more intramolecular base pairs (canonical and non-canonical) per

343 subunit were retained in the dataset. Any complex with a subunit of length >400 nucleotides

344 (almost exclusively rRNA and snRNA) or containing only subunits with length less than 25

345 nucleotides were removed from the dataset. Remaining RNA were filtered against the SPOT-RNA

346 training/validation sets (TR0/VL0/TR1/VL1) using blastn (-task blastn-short) with an e-value cutoff

347 of 0.001 and using RNA-align with a cutoff of 0.45. Identical duplicates were removed by

348 selecting structures with the largest number of base-pairing interactions. Two RNA (7r6q - rRNA

349 and 6ltp - crRNA) were also removed after manual inspection. Finally, we found that except for

350 three of the new complexes, all other complexes are homooligomers and among the original

351 complexes, only two of them are homooligomeric. Therefore, we integrated these two datasets,

352 resulting in a homo-dimer data set containing 13 complexes and a hetero-dimer data set

353 containing 15 complexes.

354 **Performance evaluation**

355 We evaluated performance using common metrics: Recall (sensitivity), Precision, and the F1

356 score. PPV/Precision is TP/(TP+FP), Sensitivity/Recall is TP/(TP+FN), and the F1 score is

357 2(Recall*Precision)/(Recall + Precision). Here, TP, FP, and FN are true positive, false positive and

358 false negative, respectively. We also calculated Matthew's correlation coefficient (MCC) to

359 provide a balanced measure as below:

360 $$MCC = \frac{TP \times TN - FP \times FN}{\sqrt{(TP+FP)(TP+FN)(TN+FP)(TN+FN)}},$$

361 where TN denotes true negatives. MCC considers true negatives (TN) and measures the

362 correlation between expected and observed classes. It ranges from 0 (no correlation) to 1

363 (highest correlation).

364 **Methods for interaction prediction**

365 We summarized the methods compared in Table 4, with detailed settings for each method

366 provided in the Supplementary method description in the Supplementary Material. As per Lai

367 and Meyer[13], we categorized the algorithms into four types: 1) 'Interaction only' methods predict

368 intermolecular hybridization, ignoring RNA secondary structures; 2) 'Accessibility' methods

369 consider RNA secondary structures using a partition function for unpaired probability; 3)

370 'Concatenation' algorithms treat two input sequences as a single chain and predict a joint

371 secondary structure; and 4) 'Complex joint' methods also predict joint secondary structures but

372 without concatenating the input sequences.

373

374 We used concatenation for comparing recent deep-learning methods with traditional free-

375 energy-based methods. When dealing with concatenated chains, we made predictions for both

376 sequence orders (AB and BA) and reported the average if probabilities were predicted. For those

377 methods providing a two-state prediction, we considered the union of base pairs predicted for

378 both sequence orders as a positive prediction (i.e. a positive prediction from either AB or BA

379 concatenation will be considered as positive).

380

381 We experimented with and without a three-nucleotide linker (AAA, UUU, CCC, or GGG) and

382 found that direct concatenation without any linker yielded slightly better results, although not

383 statistically significant compared to AAA/CCC linkers (Supplementary Table 1). Therefore, we

384 report results based on direct concatenation without any linkers.

385

386 Table 4 RRI interaction tools employed in this study for comparison, listed according to the year

387 of publication along with their categories, the use of evolution information (MSA), the algorithm,

388 and the capability of predicting intra-RNA base pairs.

Methods	Ref	Year	Category[a]	MSA[b]	Algorithms[c]	Intra-RNA base pairs[d]
RNAfoldc[e]	[45]	2004	concatenation	No	MFE	Yes
PairFold	[24]	2005	concatenation	No	MFE	Yes
RNAup	[20]	2006	accessibility	No	MFE	No

GUUGle	[14]	2006	interaction only	No	MFE	No
RNAcoFold	[25]	2006	concatenation	No	partition + MFE	Yes
NUPACK	[46]	2007	concatenation	No	MFE	No
RNAplex-c	[18]	2008	interaction only	No	MFE	No
RNAplex-a	[18]	2008	accessibility	No	MFE	No
RNAplex-cA	[18]	2008	interaction only	Yes	MFE	No
bifold	[19]	2010	complex joint	No	MFE	No
DuplexFold	[47]	2010	interaction only	No	MFE	No
PETcoFold	[29]	2011	complex joint	Yes	MFE	Yes
RNAduplex	[17]	2011	interaction only	No	MFE	No
RNAaliduplex	[17]	2011	interaction only	Yes	MFE	No
RNAmultifold	[17]	2011	concatenation	No	MFE	Yes
RIsearch	[15]	2012	interaction only	No	MFE	No
AccessFold	[23]	2016	concatenation	No	MFE	No
IntaRNA2.0	[48]	2017	accessibility	No	MFE + partition	No
SPOT-RNAc[e]	[31]	2019	concatenation	No	DL	Yes
SPOT-RNA2c[e]	[35]	2021	concatenation	Yes	DL	Yes
MXfold2c[e]	[32]	2021	concatenation	No	DL	Yes
UFoldc[e]	[33]	2022	concatenation	No	DL	Yes
EternaFoldc[e]	[49]	2022	concatenation	No	MFE	Yes

389 [a] Category: the broad category of the method (see text for more details).

390 [b]MSA—indicate whether it takes multiple sequence alignment as input.

391 [c]Algorithm: MFE: minimum free energy, Partition; partition function, DL: deep learning.

392 [d]Intra-RNA Base Pairs —whether the output of a software also contains base pairing information

393 for intramolecular interactions.

[e]c – indicates concatenation of two chains. For example, SPOT-RNAc and SPOT-RNA2c denotes SPOT-RNA and SPOT-RNA2 with sequence concatenation, respectively, to distinguish from the methods dedicated to individual chains (SPOT-RNA and SPOT-RNA2, respectively).

Homology search

For these methods that do not predicted RRI by employing a linked chain such as RNAplex-cA, PETcoFold, RNAaliduplex and SPOT-RNA2, we searched the homologs using the single chain by RNAcmap3[50] which is based on MARS database (a comprehensive database by including the RNAcentral, MG-RAST, GWH, MGnify and NCBI's nucleotide databases). For SPOT-RNA2c using a link chain, we searched the homologs with the linked chain by RNAcmap3. The median number of homologous sequences found is 1467 for single chains and 940 for linked chains.

Data and code availability

All data and codes are available at https://github.com/meilanglang/RNA-RNA-Interaction

Acknowledgement

We express our gratitude to Dr. Jaswinder Singh for valuable discussions and insights. This research received support from the National Natural Science Foundation of China (Grant # 22350710182), the Shenzhen Science and Technology Program (Grant No. KQTD20170330155106581) and benefited from access to the supercomputing resources at Shenzhen Bay Laboratory.

Conflict of Interest.

All authors declare no financial interest. Zhan and Zhou are the CEO and the chair of the scientific advisor board for Ribopeutic, respectively.

Reference

416 1. Dai, X., Zhang, S. & Zaleta-Rivera, K. RNA: interactions drive functionalities. *Mol Biol Rep* 47,
417 1413–1434 (2020).
418 2. Singh, S., Shyamal, S. & Panda, A. C. Detecting RNA–RNA interactome. *WIREs RNA* 13, e1715
419 (2022).
420 3. Gong, J., Ju, Y., Shao, D. & Zhang, Q. C. Advances and challenges towards the study of RNA-
421 RNA interactions in a transcriptome-wide scale. *Quant Biol* 6, 239–252 (2018).
422 4. Lu, Z. *et al.* RNA Duplex Map in Living Cells Reveals Higher-Order Transcriptome Structure.
423 *Cell* 165, 1267–1279 (2016).
424 5. Aw, J. G. A. *et al.* In Vivo Mapping of Eukaryotic RNA Interactomes Reveals Principles of
425 Higher-Order Organization and Regulation. *Mol Cell* 62, 603–617 (2016).
426 6. Sharma, E., Sterne-Weiler, T., O'Hanlon, D. & Blencowe, B. J. Global Mapping of Human RNA-
427 RNA Interactions. *Mol Cell* 62, 618–626 (2016).
428 7. Ziv, O. *et al.* COMRADES determines in vivo RNA structures and interactions. *Nat Methods* 15,
429 785–788 (2018).
430 8. Cai, Z. *et al.* RIC-seq for global in situ profiling of RNA–RNA spatial interactions. *Nature* 582,
431 432–437 (2020).
432 9. Xu, B. *et al.* Recent advances in RNA structurome. *Sci China Life Sci* 65, 1285–1324 (2022).
433 10. Burley, S. K. *et al.* RCSB Protein Data Bank: powerful new tools for exploring 3D structures of
434 biological macromolecules for basic and applied research and education in fundamental biology,
435 biomedicine, biotechnology, bioengineering and energy sciences. *Nucleic Acids Res* 49, D437–
436 D451 (2021).

437 11. RNAcentral Consortium. RNAcentral 2021: secondary structure integration, improved
438 sequence search and new member databases. *Nucleic Acids Res* 49, D212–D220 (2021).
439 12. Umu, S. U. & Gardner, P. P. A comprehensive benchmark of RNA–RNA interaction prediction
440 tools for all domains of life. *Bioinformatics* 33, 988–996 (2017).
441 13. Lai, D. & Meyer, I. M. A comprehensive comparison of general RNA-RNA interaction
442 prediction methods. *Nucleic Acids Res* 44, e61 (2016).
443 14. Gerlach, W. & Giegerich, R. GUUGle: a utility for fast exact matching under RNA
444 complementary rules including G-U base pairing. *Bioinformatics* 22, 762–764 (2006).
445 15. Wenzel, A., Akbasli, E. & Gorodkin, J. RIsearch: fast RNA-RNA interaction search using a
446 simplified nearest-neighbor energy model. *Bioinformatics* 28, 2738–2746 (2012).
447 16. Krüger, J. & Rehmsmeier, M. RNAhybrid: microRNA target prediction easy, fast and flexible.
448 *Nucleic Acids Res* 34, W451-454 (2006).
449 17. Lorenz, R. *et al.* ViennaRNA Package 2.0. *Algorithms Mol Biol* 6, 26 (2011).
450 18. Tafer, H. & Hofacker, I. L. RNAplex: a fast tool for RNA-RNA interaction search. *Bioinformatics*
451 24, 2657–2663 (2008).
452 19. Reuter, J. S. & Mathews, D. H. RNAstructure: software for RNA secondary structure
453 prediction and analysis. *BMC Bioinformatics* 11, 129 (2010).
454 20. Mückstein, U. *et al.* Thermodynamics of RNA-RNA binding. *Bioinformatics* 22, 1177–1182
455 (2006).
456 21. Busch, A., Richter, A. S. & Backofen, R. IntaRNA: efficient prediction of bacterial sRNA targets
457 incorporating target site accessibility and seed regions. *Bioinformatics* 24, 2849–2856 (2008).

458 22. Tafer, H., Amman, F., Eggenhofer, F., Stadler, P. F. & Hofacker, I. L. Fast accessibility-based
459 prediction of RNA-RNA interactions. *Bioinformatics* 27, 1934–1940 (2011).
460 23. DiChiacchio, L., Sloma, M. F. & Mathews, D. H. AccessFold: predicting RNA-RNA interactions
461 with consideration for competing self-structure. *Bioinformatics* 32, 1033–1039 (2016).
462 24. Andronescu, M., Zhang, Z. C. & Condon, A. Secondary structure prediction of interacting
463 RNA molecules. *J Mol Biol* 345, 987–1001 (2005).
464 25. Bernhart, S. H. *et al.* Partition function and base pairing probabilities of RNA heterodimers.
465 *Algorithms Mol Biol* 1, 3 (2006).
466 26. Kato, Y. *et al.* RactIP: fast and accurate prediction of RNA-RNA interaction using integer
467 programming. *Bioinformatics* 26, i460-466 (2010).
468 27. Kery, M. B., Feldman, M., Livny, J. & Tjaden, B. TargetRNA2: identifying targets of small
469 regulatory RNAs in bacteria. *Nucleic Acids Res* 42, W124-129 (2014).
470 28. Wright, P. R. *et al.* Comparative genomics boosts target prediction for bacterial small RNAs.
471 *Proc Natl Acad Sci U S A* 110, E3487-3496 (2013).
472 29. Seemann, S. E., Richter, A. S., Gesell, T., Backofen, R. & Gorodkin, J. PETcofold: predicting
473 conserved interactions and structures of two multiple alignments of RNA sequences.
474 *Bioinformatics* 27, 211–219 (2011).
475 30. Zhao, Y., Wang, J., Zeng, C. & Xiao, Y. Evaluation of RNA secondary structure prediction for
476 both base-pairing and topology. *Biophys Rep* 4, 123–132 (2018).
477 31. Singh, J., Hanson, J., Paliwal, K. & Zhou, Y. RNA secondary structure prediction using an
478 ensemble of two-dimensional deep neural networks and transfer learning. *Nat Commun* 10, 5407
479 (2019).

480 32. Sato, K., Akiyama, M. & Sakakibara, Y. RNA secondary structure prediction using deep
481 learning with thermodynamic integration. *Nat Commun* 12, 941 (2021).
482 33. Fu, L. *et al.* UFold: fast and accurate RNA secondary structure prediction with deep learning.
483 *Nucleic Acids Res* 50, e14 (2022).
484 34. Mao, K., Wang, J. & Xiao, Y. Length-Dependent Deep Learning Model for RNA Secondary
485 Structure Prediction. *Molecules* 27, 1030 (2022).
486 35. Singh, J. *et al.* Improved RNA Secondary Structure and Tertiary Base-pairing Prediction Using
487 Evolutionary Profile, Mutational Coupling and Two-dimensional Transfer Learning. *Bioinformatics*
488 btab165 (2021) doi:10.1093/bioinformatics/btab165.
489 36. Zhang, T. *et al.* RNAcmap: A Fully Automatic Pipeline for Predicting Contact Maps of RNAs by
490 Evolutionary Coupling Analysis. *Bioinformatics* btab391 (2021)
491 doi:10.1093/bioinformatics/btab391.
492 37. Gong, S., Zhang, C. & Zhang, Y. RNA-align: quick and accurate alignment of RNA 3D
493 structures based on size-independent TM-scoreRNA. *Bioinformatics* 35, 4459–4461 (2019).
494 38. Antonov, I. V., Mazurov, E., Borodovsky, M. & Medvedeva, Y. A. Prediction of lncRNAs and
495 their interactions with nucleic acids: benchmarking bioinformatics tools. *Briefings in*
496 *Bioinformatics* 20, 551–564 (2019).
497 39. Szikszai, M., Wise, M., Datta, A., Ward, M. & Mathews, D. H. Deep learning models for RNA
498 secondary structure prediction (probably) do not generalize across families. *Bioinformatics* 38,
499 3892–3899 (2022).
500 40. Qiu, X. Sequence similarity governs generalizability of de novo deep learning models for RNA
501 secondary structure prediction. *PLOS Computational Biology* 19, e1011047 (2023).

41. Improved prediction of protein-protein interactions using AlphaFold2 | Nature Communications. https://www.nature.com/articles/s41467-022-28865-w.

42. Lu, X.-J., Bussemaker, H. J. & Olson, W. K. DSSR: an integrated software tool for dissecting the spatial structure of RNA. *Nucleic Acids Res* 43, e142 (2015).

43. Li, W. & Godzik, A. Cd-hit: a fast program for clustering and comparing large sets of protein or nucleotide sequences. *Bioinformatics* 22, 1658–1659 (2006).

44. Zheng, J., Xie, J., Hong, X. & Liu, S. RMalign: an RNA structural alignment tool based on a novel scoring function RMscore. *BMC Genomics* 20, 276 (2019).

45. Mathews, D. H. *et al.* Incorporating chemical modification constraints into a dynamic programming algorithm for prediction of RNA secondary structure. *Proc Natl Acad Sci U S A* 101, 7287–7292 (2004).

46. Dirks, R. M., Bois, J. S., Schaeffer, J. M., Winfree, E. & Pierce, N. A. Thermodynamic Analysis of Interacting Nucleic Acid Strands. *SIAM Rev.* 49, 65–88 (2007).

47. Reuter, J. S. & Mathews, D. H. RNAstructure: software for RNA secondary structure prediction and analysis. *BMC Bioinformatics* 11, 129 (2010).

48. Mann, M., Wright, P. R. & Backofen, R. IntaRNA 2.0: enhanced and customizable prediction of RNA–RNA interactions. *Nucleic Acids Research* 45, W435–W439 (2017).

49. Wayment-Steele, H. K. *et al.* RNA secondary structure packages evaluated and improved by high-throughput experiments. *Nat Methods* 19, 1234–1242 (2022).

50. Chen, K., Litfin, T., Singh, J., Zhan, J. & Zhou, Y. MARS and RNAcmap3: The Master Database of All Possible RNA Sequences and Its Integration with RNAcmap for RNA Homology Search. *Genomics, Proteomics, & Bioinformatics*, in press (2024).

524

525